Acta Biochim Biophys Sin, 2015, 47(9), 730–740
doi: 10.1093/abbs/gmv061
Advance Access Publication Date: 2 July 2015
Original Article

Original Article

Mitochondrial fusion/fission process involved in the improvement of catalpol on high glucose-induced hepatic mitochondrial dysfunction

Zhimeng Xu[1], Luyong Zhang[1,2], Xiaojie Li[1], Zhenzhou Jiang[1,2], Lixin Sun[1,2], Guolin Zhao[1], Guohua Zhou[3], Heran Zhang[4], Jing Shang[1,2,*], and Tao Wang[1,2,*]

[1]Jiangsu Center of Drug Screening, China Pharmaceutical University, 24 Tong Jia Xiang, Nanjing 210009, China, [2]Jiangsu Center for Pharmacodynamics Research and Evaluation, China Pharmaceutical University, Nanjing 210009, China, [3]Qinghai Yangzong Pharmaceutial Co., Ltd, Xining 810003, China, and [4]Tianjin Institute of Pharmaceutical Research, Tianjin 300193, China

*Correspondence address. Tel: +86-25-83271043; Fax: +86-25-83271142; E-mail: shangjing21cn@163.com (J.S.)/wangtao1331@126.com (T.W.)

Received 10 March 2015; Accepted 4 May 2015

Abstract

Catalpol, an iridoid glycoside, has been shown to exert hypoglycemic effect by rescuing mitochondrial function, but the detailed mechanism remains unclear yet. In this study, the effect and mechanism of catalpol on the hepatic mitochondria under diabetic conditions were further examined. Oral administration of catalpol significantly reduced the blood glucose, triglyceride, and cholesterol levels in high-fat diet- and streptozotocin-induced diabetic mice. Additionally, catalpol attenuated the decrease in liver mitochondrial ATP content resulting from diabetes. Furthermore, the number of mitochondria possessing a long size was increased in catalpol-treated mice. Interestingly, the catalpol-induced recovery of mitochondrial function was associated with decreased fission protein 1 and dynamin-related protein 1 expression as well as increased mitofusin 1 expression in the liver. In HepG2 cells, catalpol alleviated the decrease of ATP content and mitochondrial membrane potential, and the increase of reactive oxygen species formation induced by high glucose. MitoTracker Green stain shows that the tubular feature of mitochondria was maintained when cells were treated with catalpol. Catalpol also decreased fission protein 1 and dynamin-related protein 1 expression and increased mitofusin 1 expression in HepG2 cells. The present results suggest that catalpol can ameliorate hepatic mitochondrial dysfunction under a diabetic state, and this may be related to its regulation of mitochondrial fusion and fission events.

Key words: catalpol, mitochondria, fusion/fission, liver, diabetic

Introduction

The liver is one of the major organs affecting and being affected by diabetes and hyperglycemia. Type 2 diabetes mellitus is defined by an increased rate of hepatic glucose production that contributes to fasting hyperglycemia [1]. In particular, increased endogenous glucose production can be accounted by increased rate of hepatic gluconeogenesis [2]. Chronically elevated blood glucose also has a significant impact on the liver itself. Previous research has shown that the expressions of proteins involved in transcriptional control, signal transduction, redox regulation, and cytoskeleton regulation were significantly altered after treatment of liver cells with high glucose [3]. Furthermore, depletion in the expressions and activities of antioxidant

enzymes was observed in primary rat hepatocytes under high glucose stress [4].

In the eukaryotic cells, mitochondria carry out multiple interconnected functions, such as producing ATP and many biosynthetic intermediates, while also regulating the communication between cells and tissues. It is therefore not surprising that mitochondrial dysfunction is a common hallmark of a myriad of diseases, including neurodegenerative and metabolic disorders [5]. As reviewed by Aparajita and Kavitha [6], hyperglycemia-induced changes in mitochondria, such as decreased oxidative phosphorylation, increased oxidative stress, and ultrastructural abnormalities, play a crucial role in promoting liver injury. However, evidence of morphological changes of mitochondria in hepatocytes has drawn much attention. Increased level of fragmented mitochondria was related to reduced fuel oxidation and increased oxidative stress in hepatocytes from diabetic rats [7]. Moreover, hypertrophic mitochondria with increased number of irregular cristae and reduced matrix electron density were observed in liver of critically ill diabetic patients [8]. Nevertheless, the research related to these changes in the mitochondria of diabetic liver cells is limited, and the mechanism requires clarification.

Fragmentation or elongation of mitochondria is determined by the fission and fusion events that can be influenced by metabolic conditions [9]. Cells exposed to a nutrient-rich environment tend to keep their mitochondria in a separated (fragmented) state, whereas the mitochondria in cells under starvation tend to remain in the connected (elongated) state for a longer duration. In mammals, mitochondrial fusion is regulated by mitofusins (Mfn1 and Mfn2) and optic atrophy gene 1 (Opa1), while mitochondrial fission is mediated by fission protein 1 (Fis1) and dynamin-related protein 1 (Drp1) [10]. Activating fusion or inhibiting fission was reported to counteract many of the disease phenotypes related to insulin resistance and diabetes [11]. Furthermore, the idea that the disruption of mitochondrial dynamics underlies the pathogenesis of diabetic liver disease is gaining support. Enhanced fission machinery and decreased mitochondrial respiratory capacity have been found in the livers of db/db mice and high-fat diet (HFD) rats [12,13].

Catalpol, an iridoid glucoside found in the root of *Rehmannia glutinosa*, was reported to have a hypoglycemic effect by promoting the synthesis of hepatic glycogen [14]. Studies in rotenone-treated mice have shown that catalpol treatment can increase complex I, superoxide dismutase (SOD), and glutathione peroxidase activities, but reduce lipid peroxidation and lead to loss of mitochondrial membrane potential [15]. Our previously study has revealed that catalpol can rescue mitochondrial ultrastructure and improve mitochondrial function in the skeletal muscle of diabetic mice [16]. To the best of our knowledge, no study has been carried out on the effects of catalpol on mitochondrial function of liver cells.

In this study, we sought to investigate the effects of catalpol on hepatic mitochondrial function under the diabetic condition and further elucidate the mechanism of action. It was found that catalpol ameliorates mitochondrial dysfunction in HFD/streptozotocin (STZ)-induced diabetic mice and glucose-treated HepG2 cells, and this effect may be related to the regulation of catalpol on mitochondrial fusion and fission events.

Materials and Methods

Materials

Catalpol (>95% purity) was a gift from Qinghai Yangzong Pharmaceutical Co., Ltd (Qinghai, China). STZ was purchased from Sangon Biotech Co., Ltd (Shanghai, China); metformin (>99.8% purity) was made in Sino-American Shanghai Squibb Co., Ltd (Shanghai, China); high-fat diet (30% fat + 70% standard chow) was obtained from Nanjing Jiangning Qinglongshan Animal Farms (Nanjing, China). Dulbecco's modified Eagle's medium (DMEM) and fetal bovine serum were purchased from Invitrogen (Shanghai, China). 2,7-Dichlorofluorescein diacetate (DCFH-DA) was purchased from Beyotime (Haimen, China). All other reagents were of analytical grade.

Animal model

All experimental procedures were conducted in conformity with institutional guidelines for the care and use of laboratory animals in China. Six-week-old male C57BL/6J mice (weight: 18 ± 2 g) were from Peking University Medical Laboratory Animal Center (Beijing, China). The modeling, grouping, and dosing methods were consistent with our previous study [16]. Finally, mice were divided into six groups (n = 8), i.e. control group, HFD- and STZ-induced diabetic group, catalpol 50, 100, and 200 mg/kg group, and metformin 200 mg/kg group. Both catalpol and metformin were dissolved in distilled water. The dose of metformin used was found in Ref. [17].

At the end of the study, animals were fasted overnight and blood samples were collected from the tail vein. Livers were immediately separated; some were used for the isolation of mitochondria or the detection of MnSOD activity, and others were stored in liquid nitrogen until further analysis.

Fasting blood glucose, triglyceride, and cholesterol

The collected blood samples were subject to centrifugation at 2000 *g* for 10 min and then used for the estimation of serum glucose, triglyceride, and cholesterol levels by using commercial kits (Whitman, Nanjing, China).

Liver mitochondria preparation

Liver mitochondria were isolated by Tissue Mitochondria Isolation Kit (Beyotime) according to the manufacturer's instructions. In brief, 100 mg of liver tissue was put into a tube placed on ice. Then, the liver tissue was cut into small pieces and homogenized in a Potter-Elvehjem tissue grinder vessel with 1 ml of buffer provided in the kit. The homogenate was then centrifuged at 600 *g* for 5 min at 4°C, and the resulting supernatant was further centrifuged at 11,000 *g* for 10 min at 4°C. The pellet was collected as mitochondria and suspended in 40 μl of mitochondrial storage fluid provided in the kit. Liver mitochondrial protein concentrations were measured with the BCA Protein Assay Kit (Beyotime).

Determination of liver mitochondrial ATP content

Total ATP content was determined using the Enliten™ ATP Assay system with bioluminescence detection kit (Promega, Madison, USA) in the isolated hepatic mitochondria. Mitochondria were dissolved in ATP-free water, then vortexed. Then, ATP was measured according to the manufacturer's instruction. Briefly, samples were neutralized to pH 7.75, and a 2-s delay time after 100 μl of rL/L reagent injection was used. Light outputs were measured by a luminometer within 10 s and compared with an ATP standard curve to calculate ATP content.

Determination of liver mitochondrial DNA copy number

Mitochondrial DNA (mtDNA) content was quantified by quantitative real-time polymerase chain reaction (qPCR) according to the method described by Zhou *et al.* [18]. Total DNA was extracted with the QIAamp DNA isolation kit (Qiagen, Dusseldorf, Germany). 16S rRNA

and Hexokinase 2 were used to represent mtDNA and nuclear DNA (nDNA), respectively. The primers used in this study were as following: 16S rRNA gene: sense primer, 5′-CCGCAAGGGAAAGATGA AAGAC-3′; antisense primer: 5′-TCGTTTGGTTTCGGGGTTTC-3′; Hexokinase 2 gene: sense prime, 5′-GCCAGCCTCTCCTGATT TTAGTGT-3′ and antisense primer, 5′-GGGAACACAAAAGACC TCTTCTGG-3′. A total volume of 20 µl mixture including DNA (10 ng) and 1 × SsoFast EvaGreen supermix (10 µl) were placed in 96-well plates. PCR procedure were as follows: initial holding at 95° C for 30 s, followed by 40 cycles of 5 s at 95°C and a final extension at 60°C for 10 s. The threshold cycle number values of mitochondrial and nuclear products were performed separately. The relative mtDNA content (mtDNA/nDNA) was calculated with the following equation: relative copy number (Rc) = $2^{\Delta Ct}$, where $\Delta Ct = Ct^{nDNA} - Ct^{mtDNA}$. The measurement of melting temperature analysis was performed in triplicate for each DNA sample.

Electron microscopy

Conventional electron microscopy (EM) technique was used as previously described [19]. Transmission EM was performed with a JEM-1010 transmission electron microscope (JEOL, Tokyo, Japan). Ten digital photomicrographs were taken randomly from each sample at 30,000× and 80,000× magnification.

Morphometric analysis

For each animal, three different fields were quantified at 30,000× magnification. The diameter of each mitochondrion was drawn interactively using ImageJ analysis software. The numbers of total mitochondria were determined.

Determination of liver manganese SOD activity

One hundred milligrams of fresh liver tissues were homogenized in physiological saline (w/w, 1:9) at 4°C, and the homogenate was centrifuged at 3500 *g* for 10 min. The MnSOD activity in the supernatant was measured using a MnSOD Assay Kit (Beyotime) according to the manufacturer's instructions. This MnSOD assay uses the water-soluble tetrazolium salt WST-1, which forms a dye upon reaction with a superoxide anion. MnSOD activity was spectrophotometrically detected at 438 nm and was expressed as the percentage of the MnSOD activity in the control sample.

Cell culture

Human hepatoma HepG2 cells were cultured in DMEM containing normal glucose (5.5 mM D-glucose), supplemented with 10% fetal bovine serum, 100 U/ml penicillin, and 0.1 mg/ml streptomycin at 37°C in a humidified 5% CO_2 incubator. The cells were grown to 70% confluence and then pre-incubated in serum-free medium for 12 h prior to treatment.

HepG2 cells were grouped as follows: 5.5 mM normal glucose group (NG), 30 mM high glucose group (HG), 30 mM high glucose + 2 mM metformin treatment group (HMG), and 30 mM high glucose + 50 µM catalpol treatment group (HCG). High glucose modeling time and catalpol concentration were selected from previous experiments (data not shown), and the concentration of metformin used was found in Ref. [20].

Reactive oxygen species generation assay

Changes in intracellular reactive oxygen species (ROS) levels were determined by measuring the oxidative conversion of cell permeable DCFH-DA with a FACSCalibur flow cytometer. HepG2 cells (1×10^6 cells/ml) cultured in 6-well dishes were collected after digestion and incubated in 1 ml of DMEM containing DCFH-DA dye (10 µM) at 37° C for 20 min. Then, the cells were centrifuged at 600 *g* for 4 min at 4° C and were subsequently washed and suspended in 0.5 ml of DMEM. The fluorescence of the cell suspension was measured and analyzed using flow cytometry. When DCF is oxidized by ROS, it emits green fluorescence at 510–540 nm after excitation at 488 nm with an argon ion laser. The levels of intracellular ROS were determined by comparing the changes in fluorescence intensity of treated cells vs. control cells.

Determination of intracellular ATP content

ATP content was measured using a CellTiter-Glo® 2.0 Assay Kit (Promega) according to the manufacturer's instructions. Cells (5×10^3) were seeded into 96-well plates (Corning, New York, USA) and all treatments were performed in three independent experiments.

Mitochondrial membrane potentials

The mitochondrial membrane potential ($\Delta\Psi_m$) of treated HepG2 cells was evaluated using a FACSCalibur flow cytometer (Becton Dickinson, San Jose, USA) and a JC-1 Mitochondrial Membrane Potential Detection Kit (Beyotime) as previously described [21]. Cell treated with 10 µM carbonyl cyanide m-chlorophenylhydrazone (CCCP) was used as negative control. CCCP is a protonophore which can cause dissipation of $\Delta\Psi$m. The cells were stained with 2 mM JC-1 for 30 min at 37°C. Fluorescence intensities were determined using flow cytometry.

Mitochondrial staining

After being incubated with 30 mM D-glucose for 24 h and treated with drugs, cells were stained with 100 nM Mito Tracker Green (Molecular Probes, Carlsbad) for 15 min at 37°C. Then, mitochondria were visualized by a confocal microscope with a 100× objective lens.

RNA isolation and qPCR

qPCR assays were performed as previously described by Wang *et al.* [22]. Total RNA was isolated from mouse liver tissue or HepG2 cells using Trizol reagent (Vazyme, Nanjing, China) according to the manufacturer's instructions. Two micrograms of total RNA of each sample was reverse transcribed into cDNA using the HiscriptTM Q RT SuperMix for qPCR kit (Vazyme). The resulting cDNAs were amplified using a SYBR Green Master Mix Kit in iQ™5 real-time PCR detection system (Bio-Rad Laboratories, Hercules, USA). The procedure used was as follows: 95°C for 30 s, and 40 cycles of 95°C for 5 s, and 60°C for 10 s. The primers used in the PCR are listed in **Table 1**. Gene expression levels were calculated using the $2^{-\Delta\Delta Ct}$ method.

Western blot analysis

Proteins were extracted from liver tissue and HepG2 cells as described by Chung *et al.* [23]. Proteins (80 µg) were separated by sodium dodecyl sulfate–polyacrylamide gel electrophoresis on 10% or 15% separating gel, transferred to PVDF membranes, and then blocked for 1 h at room temperature with 5% non-fat milk solution in Tris-buffered saline containing 0.1% Tween-20. Western blot analyses were performed using the following primary antibodies: anti-dynamin-related protein 1 (1:1000; Cell Signaling Technology, Danvers, USA), anti-mitofusin 1 (1:500; Santa Cruz Biotechnology, Dallas, USA), and anti-fission-1 protein (1:500; Santa Cruz

Table 1. Primers used for real-time RT-PCR

Gene name	Forward (5′ → 3′)	Reverse primer (5′ → 3′)
Homo UCP2	GCTTTGAAGAACGGGACACC	ATGATGCTGATTTCCTGCTACG
Homo SOD2	TGGCTAAGAAGGCGATTACTGC	TCTCCGAGATAGCACCTCACC
Homo SIRT3	ACCCAGTGGCATTCCAGAC	GGCTTGGGGTTGTGAAAGAAG
Homo Mfn1	TGGCTAAGAAGGCGATTACTGC	TCTCCGAGATAGCACCTCACC
Homo Mfn2	CTCTCGATGCAACTCTATCGTC	TCCTGTACGTGTCTTCAAGGAA
Homo Opa1	TGTGAGGTCTGCCAGTCTTTA	TGTCCTTAATTGGGGTCGTTG
Homo Fis1	GTCCAAGAGCACGCAGTTTG	ATGCCTTTACGGATGTCATCATT
Homo Drp1	CTGCCTCAAATCGTCGTAGTG	GAGGTCTCCGGGTGACAATTC
Homo GAPDH	GGAGCGAGATCCCTCCAAAAT	GGCTGTTGTCATACTTCTCATGG
Mus UCP2	ATGGTTGGTTTCAAGGCCACA	TTGGCGGTATCCAGAGGGAA
Mus SOD2	CCAAGGGAGATGTTACAACTCAG	GGGCTCAGGTTTGTCCAGAA
Mus SIRT3	GGCTCTATACACAGAACATCGAC	TAGCTGTTACAAAGGTCCCGT
Mus Mfn1	ATGGCAGAAACGGTATCTCCA	GCCCTCAGTAACAAACTCCAGT
Mus Mfn2	AGAACTGGACCCGGTTACCA	CACTTCGCTGATACCCCTGA
Mus Opa1	TGGAATACAAAGAAACGTACCGC	GGGCAGGATGATGTGAACGA
Mus Fis1	AGAGCACGCAATTTGAATATGCC	ATAGTCCCGCTGTTCCTCTTT
Mus Drp1	CCTCAGATCGTCGTAGTGGGA	GTTCCTCTGGGAAGAAGGTCC
Mus GAPDH	AGGTCGGTGTGAACGGATTTG	GGGGTCGTTGATGGCAACA

Homo, human; Mus, mouse.

Biotechnology). After extensive washing, membranes were incubated with the appropriate horseradish peroxidase conjugated secondary antibodies (1:20,000). Finally, blots were detected by using an enhanced chemiluminiscence kit. Densitometric analysis of the bands for the expression of protein was done with Densitograph Software (Bio-Rad).

Statistical analysis

All values were expressed as the mean ± SEM of the samples for each group. Statistical comparisons were performed using one-way analysis of variance (ANOVA) followed by Dunnett's test. The differences were considered significant when $P < 0.05$.

Results

Effects of catalpol on body weight and serum parameters in diabetic mice

Our results showed that catalpol slightly increased the body weight of the HFD/STZ-diabetic mice and significantly reduced the blood glucose, triglyceride, and cholesterol levels of HFD/STZ-diabetic mice (**Supplementary Table S1**), which were in agreement with our previous study [16].

Effects of catalpol on ATP content in liver tissue of diabetic mice

Figure 1 shows that liver mitochondrial ATP content was reduced by ~80% in the livers of HFD/STZ-diabetic mice when compared with the control ($P < 0.01$), which was reversed by the administration of catalpol or metformin ($P < 0.01$).

Effects of catalpol on mtDNA in liver tissue of diabetic mice

Figure 2 shows the copy number of mtDNA in the livers of control and model mice. The mtDNA copy number in HFD/STZ-diabetic mice was not significantly different from that in control mice. The number of mtDNA in the catalpol-treated group shows a slight but not significant increase compared with that in the HFD/STZ-diabetic group. In addition, no significant change was observed in the metformin-treated group when compared with the HFD/STZ-diabetic group.

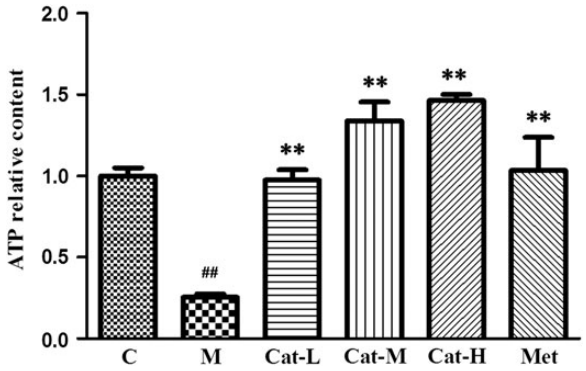

Figure 1. Catalpol increases ATP content in isolated mitochondria from HFD/STZ-induced mice liver C, control mice; M, model HFD/STZ mice; Cat-L, Cat-M, and Cat-H, HFD/STZ mice orally treated with 50, 100, and 200 mg/kg catalpol, respectively; Met, HFD/STZ mice orally treated with 200 mg/kg metformin. Data were presented as the mean ± SEM ($n = 8$). One-way ANOVA was followed by Dunnett's test. $^{\#\#}P < 0.01$ vs. control group; $^{**}P < 0.01$ vs. model group.

Mitochondrial ultrastructure changes in liver tissue of diabetic mice

Because changes in mitochondrial function are always associated with changes in mitochondrial morphology, EM observations were performed to evaluate ultrastructural features in the control group, HFD/STZ-diabetic group, and 200 mg/kg catalpol group (**Fig. 3**). In the control mice, liver mitochondria were distributed with normal size, well-defined membranes, and well-delineated cristae. In contrast, the livers of the diabetic mice contained numerous small, round, and fragmented mitochondria. After 200 mg/kg catalpol administration,

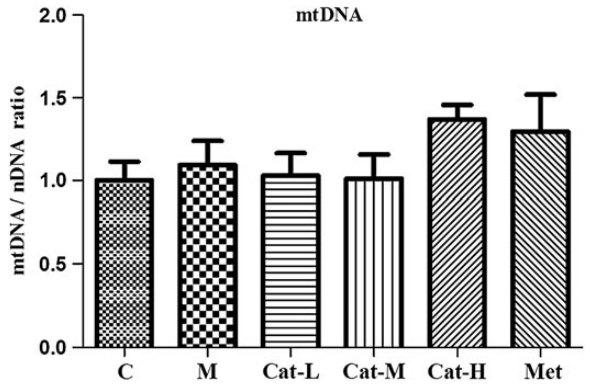

Figure 2. Effect of catalpol on DNA copy number of hepatic mitochondria in HFD/STZ-induced mice C, control mice; M, model HFD/STZ mice; Cat-L, Cat-M, and Cat-H, HFD/STZ mice orally treated with 50, 100, and 200 mg/kg catalpol, respectively; Met, HFD/STZ mice orally treated with 200 mg/kg metformin. Data were presented as the mean ± SEM ($n = 8$). One-way ANOVA was followed by Dunnett's test.

liver mitochondria were larger and less swollen, and had well-organized cristae. Analysis of the number of mitochondria showed that there was no significant difference among the groups (**Fig. 3G**). To examine the distribution of mitochondrial length, liver mitochondria were divided into three length ranges, and our results revealed that HFD/STZ-diabetic mice exhibited the highest percentage of short mitochondria. Catalpol administration can significantly increase the length of mitochondria (**Fig. 3H**).

Changes of hepatic MnSOD activity and expressions of SOD2, uncoupling protein 2, and sirtuin 3

To investigate the effect of catalpol on mitochondrial antioxidative capacity, the hepatic MnSOD activity and mitochondrial SOD2, uncoupling protein 2 (UCP2), and sirtuin 3 (SIRT3) expressions were detected (**Fig. 4A,B**). There was no significant difference in the MnSOD activity or in the expressions of SOD2, UCP2, and SIRT3 between HFD/STZ-diabetic mice and the control mice. In the 100 mg/kg catalpol ($P < 0.05$) and 200 mg/kg catalpol ($P < 0.01$) treatment groups, the activity of MnSOD was increased significantly when compared with the HFD/STZ-diabetic group. However, the expressions of SOD2, UCP2, and SIRT3 were not changed by catalpol treatment (**Fig. 4A,B**). Metformin also just significantly increased the activity of MnSOD ($P < 0.01$) when compared with the HFD/STZ-diabetic group (**Fig. 4A,B**).

Mitochondrial fission and fusion in diabetic mice

The expressions of proteins that regulate mitochondrial fusion and fission events were examined. The mRNA (**Fig. 5A**) and protein level (**Fig. 5C,D**) of Fis1 were markedly increased, but the mRNA (**Fig. 5B**) and protein level (**Fig. 5C,D**) of Mfn1 were significantly reduced in the HFD/STZ-diabetic group compared with the control group. After catalpol treatment, the Fis1 expression was significantly suppressed while the Mfn1 expression was increased in a dose-dependent manner. In the HFD/STZ-diabetic mice, the Drp1 mRNA level was decreased (**Fig. 5A**), but its protein level was remarkably increased (**Fig. 5C,D**). However, administration of catalpol could significantly increase Drp1 mRNA expression and decrease its protein level in liver. However, metformin decreased Fis1 and Drp1 expressions but increased Mfn1 expression in the liver. And the expressions of Mfn2 and Opa1 were not significantly different between these groups (**Fig. 5B**).

Improvement of mitochondrial dysfunction in HepG2 cells

To examine the defensive effect of catalpol against oxidative attack, the ROS level in cells was detected. As shown in **Fig. 6A**, high glucose induced a marked increase in ROS production ($P < 0.01$), while treatment with catalpol ($P < 0.05$) or metformin ($P < 0.05$) resulted in a significant suppression of ROS formation. However, no significant changes were observed in the expressions of UCP2, SOD2, and SIRT3 between the high glucose-treated HepG2 cells and normal cells (**Fig. 6B**). Catalpol stimulated SOD2 expression, but did not influence UCP2 and SIRT3 mRNA levels (**Fig. 6B**). Metformin can promote the expressions of UCP2 and SOD2 ($P < 0.05$) and it did not affect SIRT3 mRNA level significantly (**Fig. 6B**).

Mitochondrial hyperpolarization may have inhibitory effects on ATP synthesis. Indeed, we observed a decrease in the ATP content of the high glucose-treated cells compared with that of the control cells (**Fig. 6C**). Catalpol or metformin administration efficiently restored the ATP content ($P < 0.05$).

By using a specific probe (JC-1) of $\Delta\Psi_m$, we detected an increase in red fluorescence and a significant decrease in green fluorescence in high glucose-treated HepG2 cells, indicating that hyperglycemia exposure hyperpolarized the mitochondrial membrane (**Fig. 6D**). Nevertheless, the mitochondrial membrane potential was increased by catalpol or metformin.

Effects of catalpol on mitochondrial morphology of HepG2 cells

MitoTracker Green staining revealed that HepG2 cells exhibited an interconnected network of tubular and elongated structures (**Fig. 7A**). In contrast, mitochondrial morphology was shifted toward a fragmented and discontinuous network (**Fig. 7B**) when cells were treated with high glucose. However, the tubular feature was maintained when cells were treated with catalpol or metformin (**Fig. 7C,D**).

Mitochondrial fission and fusion in HepG2 cells

The expressions of proteins involved in mitochondrial fission and fusion were also examined in HepG2 cells. It was found that only Mfn1 mRNA level was decreased by high glucose, whereas other genes were unaffected (**Fig. 8A,B**). Treatment with catalpol or metformin notably increased the Mfn1 expression (**Fig. 8B**). When the protein levels of Fis1, Drp1, and Mfn1 in total protein extracts from HepG2 cells were analyzed by western blotting, it was found that the protein levels of Fis1 and Drp1 were prominently increased in HepG2 cells treated with high glucose, while the protein level of Mfn1 was obviously decreased (**Fig. 8C,D**). These changes were reversed by catalpol or metformin treatment.

Discussion

Functional perturbations in mitochondria have been identified to affect the cause and complications of diabetes [24]. However, investigations of mitochondrial dysfunction in diabetes mellitus were primarily focused on skeletal muscle and fat tissues, whereas few studies are focused in the liver [25]. In fact, hepatic mitochondrial dysfunction is closely related to the abnormal metabolism of glucose and lipids in diabetes, and it may be the underlying cause of hepatic insulin

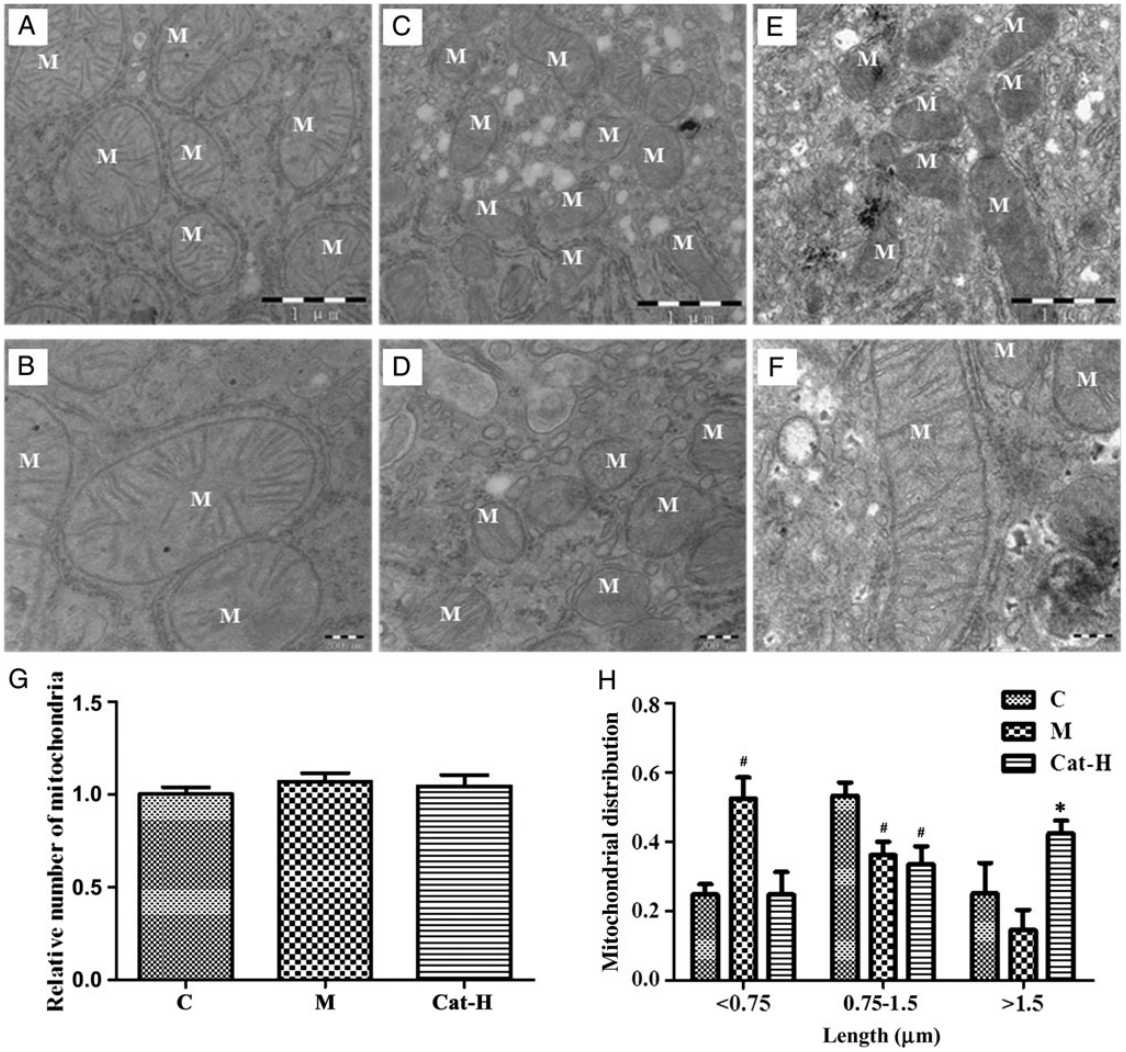

Figure 3. Hepatic mitochondrial morphology changes in HFD/STZ-induced mice with or without catalpol revealed by transmission EM Representative images to compare the differences between the mitochondria of different groups. (A,B) Control group (A: 30,000× and B: 80,000×). (C,D) Model HFD/STZ group (C: 30,000× and D: 80,000×). (E,F) Catalpol-treated (200 mg/kg) group (E: 30,000× and F: 80,000×). The white letter 'M' represents mitochondria. (G) The relative number of mitochondria. (H) The distribution of mitochondrial length. Data were presented as the mean ± SEM ($n = 8$). One-way ANOVA was followed by Dunnett's test. $^{\#}P < 0.05$ vs. control group; $^{*}P < 0.05$ vs. model group.

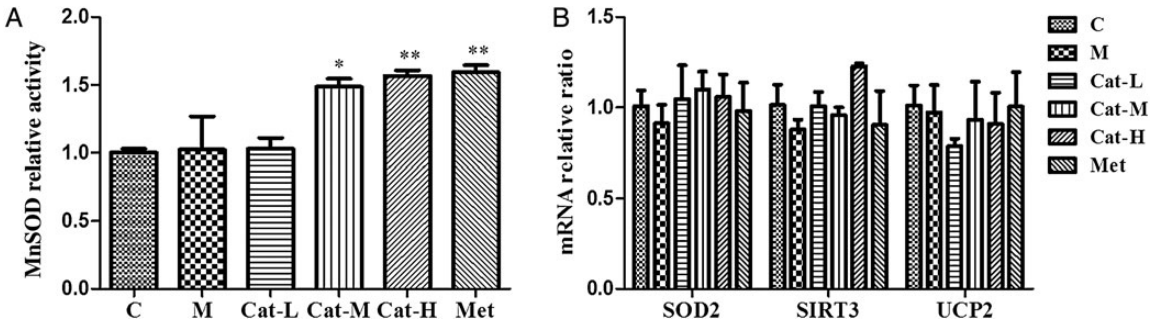

Figure 4. Effect of catalpol on hepatic MnSOD activity and gene expressions of hepatic SOD2, UCP2, and SIRT3 in HFD/STZ-induced mice (A) MnSOD activity in liver of different groups. (B) SOD2, UCP2, and SIRT3 expressions in liver of different groups. C, control mice; M, model HFD/STZ mice; Cat-L, Cat-M, and Cat-H, HFD/STZ mice orally treated with 50, 100, and 200 mg/kg catalpol, respectively; Met, HFD/STZ mice orally treated with 200 mg/kg metformin. Data were presented as the mean ± SEM ($n = 8$). One-way ANOVA was followed by Dunnett's test. $^{*}P < 0.05$, $^{**}P < 0.01$ vs. model group.

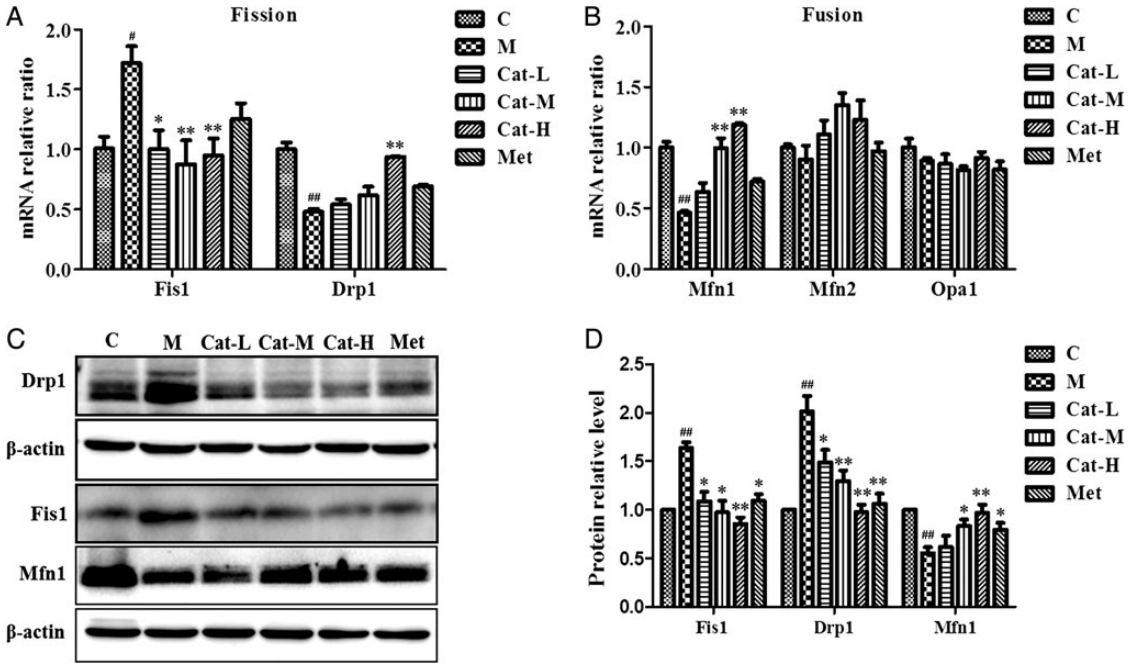

Figure 5. Expression level of genes related to hepatic mitochondrial fission and fusion in HFD/STZ-induced mice (A) mRNA expressions of Fis1 and Drp1 related to hepatic mitochondrial fission. (B) mRNA expressions of Mfn1, Mfn2, and OPA1 related to hepatic mitochondrial fusion. Data were expressed by the mean ± SE ($n = 8$). Protein levels of Drp1, Fis1, and Mfn1 were analyzed by western blotting (C) and quantified by densitometry (D) in total protein extracts from livers. Data were expressed as the mean ± SEM ($n = 3$). C, control group; M, model HFD/STZ group; Cat-L, Cat-M, and Cat-H, HFD/STZ mice orally treated with 50, 100, and 200 mg/kg catalpol, respectively; Met, HFD/STZ mice orally treated with 200 mg/kg metformin. One-way ANOVA was followed by Dunnett's test. $^{\#}P < 0.05$, $^{\#\#}P < 0.01$ vs. control group; $^{*}P < 0.05$, $^{**}P < 0.01$ vs. model group.

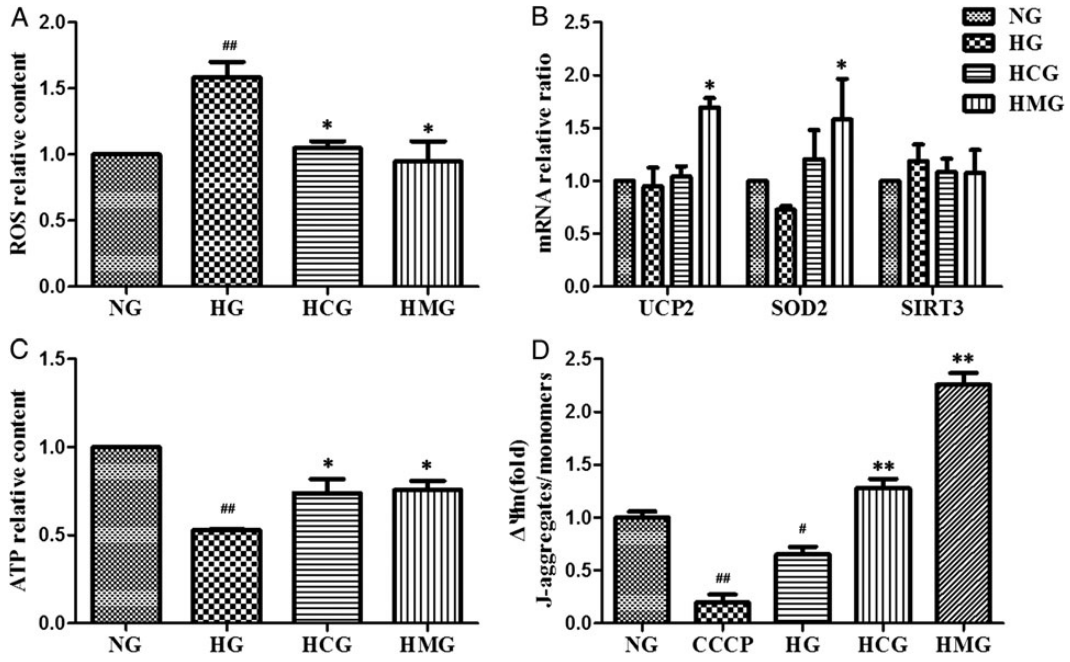

Figure 6. Effects of catalpol on mitochondria dysfunctions in HepG2 cells induced by high glucose HepG2 cells were incubated with high glucose for 24 h in the presence of the indicated concentrations 50 μM catalpol or 2 mM metformin. (A) Catalpol inhibited HG-induced generation of intracellular ROS. (B) Effect of catalpol on gene expressions of UCP2, SOD2, and SIRT3. (C) Catalpol inhibited high glucose-induced decrease of ATP content. (D) Catalpol inhibited high glucose-induced $\Delta\Psi_m$ collapse. NG, 5.5 mM normal glucose group; HG, 30 mM high glucose group; HCG, 50 μM catalpol treatment group; HMG, 2 mM metformin treatment group. Data were expressed as the mean ± SEM from three independent experiments. One-way ANOVA was followed by Dunnett's test. $^{\#}P < 0.05$, $^{\#\#}P < 0.01$ vs. control group; $^{*}P < 0.05$, $^{**}P < 0.01$ vs. model group.

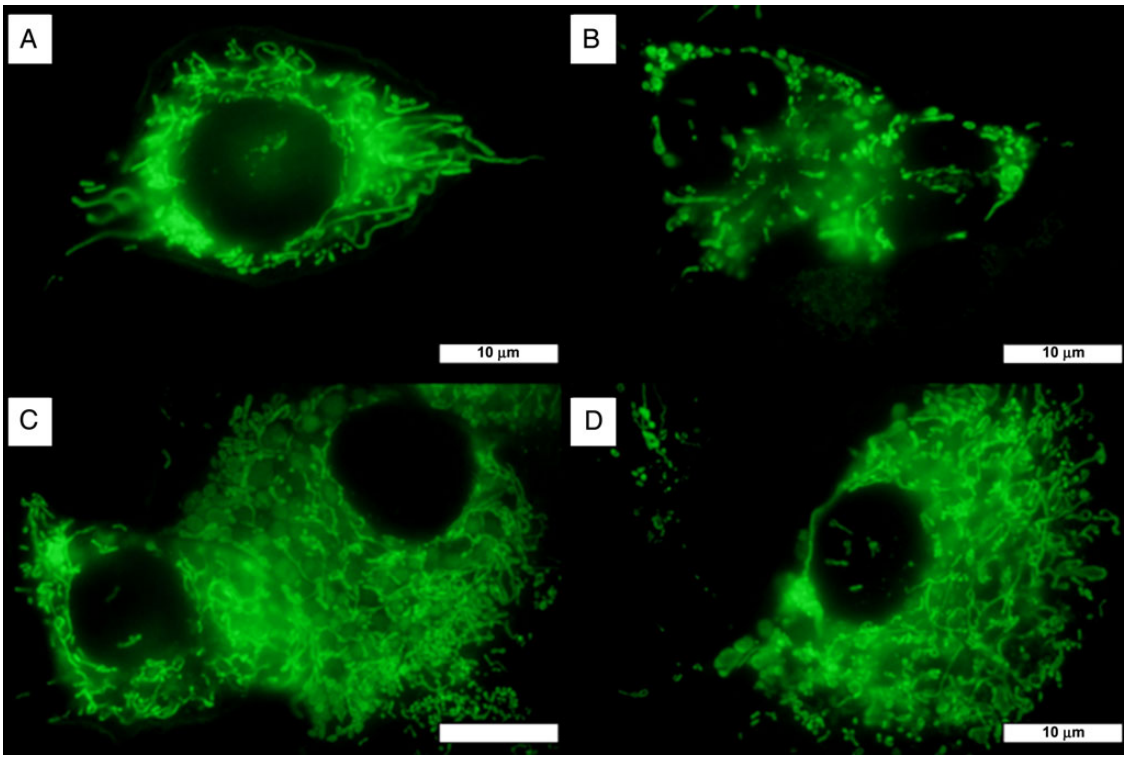

Figure 7. Mitochondrial morphology changes in HepG2 cells induced by high glucose with or without catalpol and metformin revealed by laser scanning confocal microscopy Images of HepG2 cells stained with MitoTracker Green after 24 h of high glucose with or without catalpol and metformin. Scale bar = 10 μm. (A) Normal glucose group (NG). (B) High glucose group (HG). (C) Catalpol group (HCG). (D) Metformin group (HMG).

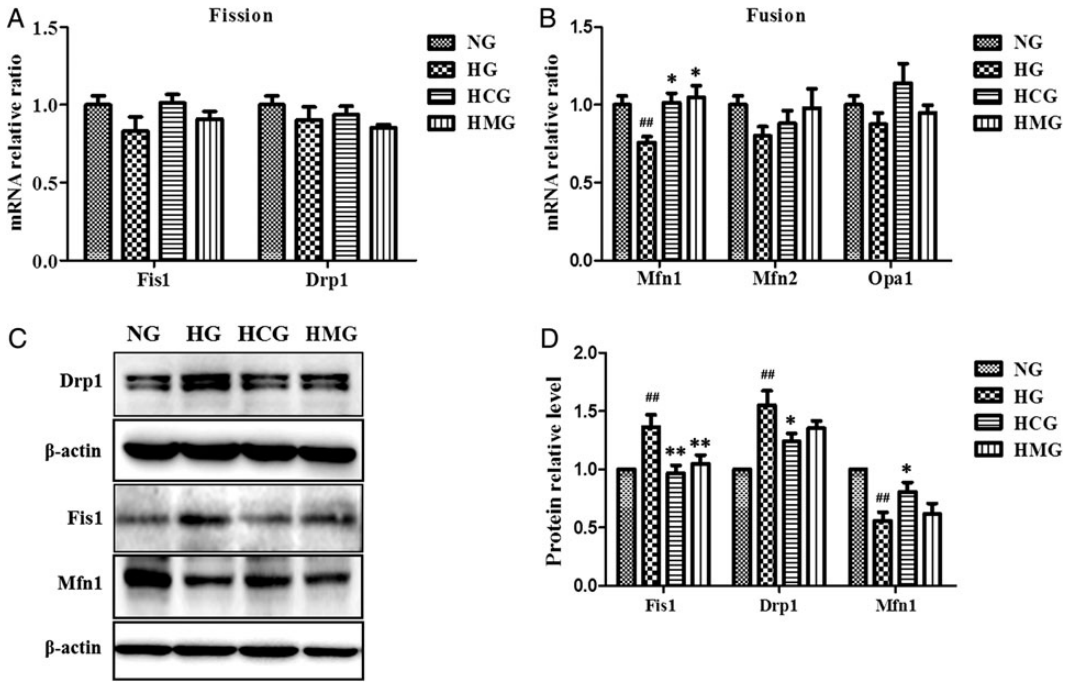

Figure 8. Expressions of genes related to mitochondrial fission/fusion in HepG2 cells (A) mRNA expressions of Fis1 and Drp1 related to mitochondrial fission in HepG2 cells. (B) mRNA expressions of Mfn1, Mfn2, and OPA1 related to mitochondrial fusion in HepG2 cells. Protein levels of Drp1, Fis1, and Mfn1 were analyzed by western blot analysis (C) and quantified by densitometry (D) in HepG2 cells. NG, 5.5 mM normal glucose group; HG, 30 mM high glucose group; HCG, 50 μM catalpol treatment group; HMG, 2 mM metformin treatment group. Data were expressed as the mean ± SEM from three independent experiments. One-way ANOVA was followed by Dunnett's test. $^{\#\#}P < 0.01$ vs. control group; $^{*}P < 0.05$, $^{**}P < 0.01$ vs. model group.

resistance [26]. Furthermore, hyperglycemia-induced mitochondrial dysfunction in liver holds importance in the context of liver injury and non-alcoholic fatty liver disease [6]. Therefore, the development of a pharmacological intervention to specifically improve liver mitochondrial dysfunction is an important issue.

Catalpol is an iridoid glycoside present in the roots of *R. glutinosa* that is widely used to treat diabetic disorders in Chinese traditional medicine. The hypoglycemic effect of catalpol has been shown to be related to increased glycogen synthesis and reduction of phosphoenolpyruvate carboxykinase expression in the liver of STZ-diabetic rats [14,27]. These results imply that catalpol could influence glucose and lipid metabolism in the liver, but its mechanism of action is still unclear. Recently, we found that oral administration of catalpol results in an increase in mitochondrial ATP content and $\Delta\Psi_m$ in the skeletal muscle of HFD/STZ-induced diabetic mice [16]. As mentioned above, mitochondria dysfunction in the liver is a more problematic lesion in diabetes mellitus, so we urgently want to know whether catalpol has regulating effects on liver mitochondria.

The main function of mitochondria in the cells is to provide ATP through oxidative phosphorylation. Our data showed decreased liver mitochondrial ATP content in HFD/STZ-diabetic mice, which is consistent with what has been previously reported in STZ-diabetic rats [25]. Catalpol administration can inhibit this decrease in a dose-dependent manner (**Fig. 1**). *In vitro*, the decreased ATP content induced by high glucose in HepG2 cells could also be prevented by catalpol (**Fig. 6C**). These results indicate that catalpol can improve hepatic mitochondrial energy synthesis.

Decreased mitochondrial antioxidative capacity and ATP synthesis has been associated with reduced mitochondrial biogenesis, and decreases in mtDNA copy number have been linked to the pathogenesis of type 2 diabetes [28,29]. In addition, our previous work revealed that the beneficial effect of catalpol on mitochondrial dysfunction in diabetic skeletal muscle was related to the promoted biosynthesis of mitochondria [16]. In the present study, we first measured the number of mtDNA in mouse liver cells. To our surprise, the results indicated that the mtDNA copy number of HFD/STZ-diabetic group mice did not decreased obviously when compared with the control mice. Furthermore, catalpol failed to show significant influence on the hepatocyte mtDNA number in diabetic mice (**Fig. 2**). As studies have showed that the compensatory ability of liver is stronger than skeletal muscle, we believe that the decrease of liver mitochondrial ATP content in our animal model may not be linked to the change of mitochondrial biogenesis [30,31]. From the TEM results with 30,000× magnification, it was also found that the number of mitochondria in catalpol administration group animal did not show significant increase compared with the HFD/STZ-diabetic group mice (**Fig. 3E**). But, the number of mitochondria with larger volume was increased, which was more obvious in the TEM results with 80,000× magnification. As shown in the **Fig. 3F**, the complete structures of mitochondria were almost maintained in catalpol treatment group. These results indicated that catalpol was involved in the regulation of mitochondria structures but not involved in mitochondrial generation in the liver cells of this animal model.

When substrates are metabolized, the mitochondrial electron transport system generates substantial superoxide derived from electron leaks [32]. In high glucose state, there is an increment of partial reduction of O_2, leading to the increased generation of free radical anion superoxides [33]. As a result, the mitochondrial antioxidant ability will be weakened and then cause decline in mitochondrial oxidative phosphorylation capacity [34]. Many studies have revealed the antioxidative activity of catalpol [35–37]. Hence, we speculate that catalpol may increase the mitochondrial antioxidative activity to regulate mitochondrial oxidative phosphorylation capacity. Superoxide, the primary ROS generated at the respiratory chain, can be converted to hydrogen peroxide. In mitochondria, this process is catalyzed by MnSOD [38]. Therefore, we examined the MnSOD activity in liver cells. In the STZ/HFD mice, the MnSOD activity did not show any significant change. This is consistent with the study of Jang *et al*. [39]. However, the detection of SOD2 RNA levels showed the same results. At the post-translational level, the deacetylation of a conserved lysine residue of murine MnSOD by the mitochondrial sirtuin SIRT3 is an important regulatory mechanism to activate the enzyme [40]. So, we measured the levels of SIRT3 mRNA. Our results suggested that the changes of SIRT3 mRNA levels were not significant. The UCPs are a family of mitochondrial transport proteins located in the inner mitochondrial membrane [41]. High transmembrane proton gradient and membrane potential of mitochondria will induce ROS production and thus oxidative damage. These ROSs may activate UCPs and therefore cause a 'mild uncoupling' and (as a negative feedback) will prevent further superoxide production and decrease oxidative damage [42]. UCP2 is the most widely distributed UCP. Several lines of evidence suggest that UCP2 is involved in the control of ROS production in mitochondria. In addition, over-expression of UCP2 prevents ROS production induced by high glucose [43]. So, the levels of UCP2 mRNA were measured. We found that the change of UCP2 mRNA level was not obvious. Therefore, the reduced liver mitochondrial ATP content in diabetic mice may not be caused by the decrease of antioxidative capactivity of mitochondria.

Current research suggests that the control of mitochondrial quality is very important to maintain the ability of ATP synthesis [44]. At the organellar level, the fission and fusion of mitochondria is the first pathway of quality control that becomes important when the molecular pathways are overwhelmed [38]. However, mitochondrial dynamics is closely related to bioenergetic efficiency and energy expenditure [9]. Furthermore, a reduction in mitochondrial fusion was considered to be a key risk factor in the development of obesity and insulin resistance [45]. Enhanced fission machinery has also been found in the liver of genetically obese and diet-induced obese animals [12,13]. In order to figure out the regulation mechanism of catalpol on hepatocyte mitochondrial ATP content, the expressions of genes related to these events were analyzed. In HFD/STZ-diabetic group, the mRNA level of Fis1 was enhanced and the mRNA level of Mfn1 was reduced (**Fig. 5A,B**), suggesting an imbalance toward mitochondrial fragmentation, which was supported by the presence of smaller mitochondria and increased presence of round mitochondria, but not the tubular ones in ultra-thin sections (**Fig. 3D**). However, the mRNA levels of mitochondrial Mfn2 and Opa1 in HFD/STZ-diabetic mice were comparable with those in the control group (**Fig. 5B**). Consistent with the results of PCR, the Mfn1 protein level in the liver of the HFD/STZ-diabetic mice was decreased, while the Fis1 protein level was increased (**Fig. 5C,D**). Treatment of HFD/STZ-diabetic mice with catalpol increased Mfn1 expression in the liver (**Fig. 5B**). Mitofusin-1 protein is a mediator of mitochondrial fusion in mammalian cells, and high levels of Mfn1 in cultured cells could lead to the formation of typical grape-like perinuclear clusters of mitochondria containing many large mitochondria around the outer edge [46]. In high glucose-treated HepG2 cells, catalpol was found to inhibit the decrease of Mfn1 (**Fig. 8B**). In addition, MitoTracker Green stain results showed that the tubular feature of mitochondria was maintained when cells were treated with catalpol (**Fig. 7C**). Therefore, our results indicate that catalpol may promote mitochondrial fusion through Mfn1. Fis1 is a protein participating in the mitochondrial fission process. Over-expression of Fis1 induced

by excess nutrients has been reported in many studies [13,47,48]. As expected, catalpol can inhibit Fis1 expression in HFD/STZ-diabetic mouse livers (**Fig. 5**) and high glucose-treated HepG2 (**Fig. 8**) cells. Surprisingly, the Drp1 mRNA expression level was decreased in HFD/STZ-diabetic animals, but the protein levels were elevated in diabetic mouse livers and high glucose-treated HepG2 cells. However, this result is in accordance with what was reported by Holmström *et al*. [12], who also showed an increase in Drp1 protein content and a decrease in Drp1 mRNA expression of the liver of db/db mice. Administration of catalpol could significantly increase Drp1 mRNA expression and decrease its protein level in liver (**Fig. 5A,C, D**) and in high glucose-treated HepG2 cells (**Fig. 8A,C,D**). As Drp1 is directly involved in the regulation of mitochondrial fission by protein forms, catalpol can inhibit mitochondrial fission through decreasing its protein expression. Thus, the enhancing effect of catalpol on diabetic mice liver ATP content is related to its regulation of mitochondrial fission/fusion process.

Because increased production of ROS in hyperglycemic conditions requires the dynamic change of mitochondrial morphology and inhibition of mitochondrial fission prevents periodic fluctuation of ROS production during high glucose exposure [47], the effect of catalpol on ROS content of high glucose-treated HepG2 cell was investigated in this study. Results showed that catalpol suppresses the generation of ROS in HepG2 cells (**Fig. 6A**). In accordance with the results in hepatocyte of diabetic mice, catalpol did not affect the expressions of SOD2, UCP2, and SIRT3 in HepG2 cells (**Figs. 4B** and **6B**). This implies that the ability of catalpol to decrease ROS may be related to its regulation of the mitochondrial fission/fusion process. Mitochondria dysfunction is also characterized by a loss of mitochondrial membrane integrity [48], and therefore we measured the change in MMP. Our data indicated that catalpol treatment caused a significant increase in MMP in HepG2 cells (**Fig. 6D**). This result suggests that catalpol can maintain the integrity of mitochondrial membrane.

In summary, catalpol was demonstrated to improve hepatic mitochondrial dysfunction induced by high glucose. Unlike promoting mitochondria synthesis in the skeletal muscle of HFD/STZ-induced diabetic mice, catalpol improved the mitochondrial function likely associated with enhancing mitochondrial fusion through Mfn1 and suppressing fission through Fis1 and Drp1 in liver. Our results illustrate a new molecular mechanism underlying the amelioration of mitochondrial dysfunction by catalpol. In this work, catalpol is shown to improve the hepatic mitochondrial function via activation of Mfn1 and inhibition of Fis1 and Drp1, indicating that catalpol and possibly its chemically modified derivatives might be potential therapeutic compounds for metabolic disorders associated with mitochondrial dysfunction.

Supplementary Data

Supplementary data is available at *ABBS* online.

Acknowledgements

The authors would like to thank Qinghai Yangzong Pharmaceutial Co., Ltd for the generous gifts of catalpol.

Funding

This work was supported by the grants from the National Natural Science Foundation of China (Nos. 81403154 and 81320108029), the National 12th Five-year Plan (No. 2012ZX09504001-001), and the 111 Project (111-2-07).

References

1. Gastaldelli A, Cusi K, Pettiti M, Hardies J, Miyazaki Y, Berria R, Buzzigoli E, *et al*. Relationship between hepatic/visceral fat and hepatic insulin resistance in nondiabetic and type 2 diabetic subjects. *Gastroenterology* 2007, 133: 496–506.
2. Magnusson I, Rothman DL, Katz LD, Shulman RG, Shulman GI. Increased rate of gluconeogenesis in type II diabetes mellitus: a ^{13}C nuclear magnetic resonance study. *J Clin Invest* 1992, 90: 1323–1327.
3. Chen JY, Chou HC, Chen YH, Chan HL. High glucose-induced proteome alterations in hepatocytes and its possible relevance to diabetic liver disease. *J Nutr Biochem* 2013, 24: 1889–1910.
4. Radhika K, Poonam K. Protective role of morin, a flavonoid, against high glucose induced oxidative stress mediated apoptosis in primary rat hepatocytes. *PLoS ONE* 2012, 7: e41663.
5. Jodi N, Anu S. Mitochondria: in sickness and in health. *Cell* 2012, 148: 1145–1159.
6. Aparajita D, Kavitha S. Hyperglycemia-induced mitochondrial alterations in liver. *Life Sci* 2010, 87: 197–214.
7. Vanhorebeek I, Ellger B, De Vos R, Boussemaere M, Debaveye Y. Tissue-specific glucose toxicity induces mitochondrial damage in a burn injury model of critical illness. *Crit Care Med* 2009, 37: 1355–1364.
8. Vanhorebeek I, De Vos R, Mesotten D, Wouters PJ, de Wolf-Peeters C. Protection of hepatocyte mitochondrial ultrastructure and function by strict blood glucose control with insulin in critically ill patients. *Lancet* 2005, 365: 53–59.
9. Liesa M, Shirihai OS. Mitochondrial dynamics in the regulation of nutrient utilization and energy expenditure. *Cell Metab* 2013, 17: 491–506.
10. Benedikt W. Mitochondrial fusion and fission in cell life and death. *Nat Rev Mol Cell Biol* 2010, 11: 872–884.
11. Civitarese AE, Ravussin E. Mitochondrial energetics and insulin resistance. *Endocrinology* 2008, 149: 950–954.
12. Holmström MH, Iglesias GE, Zierath JR, Garcia-Roves PM. Tissue-specific control of mitochondrial respiration in obesity-related insulin resistance and diabetes. *Am J Physiol Endocrinol Metab* 2012, 302: E731–E739.
13. Lionetti L, Mollica MP, Donizzetti I, Gifuni G, Sica R, Pignalosa A, Cavaliere G, *et al*. High-lard and high-fish-oil diets differ in their effects on function and dynamic behaviour of rat hepatic mitochondria. *PLoS ONE* 2014, 9: e92753.
14. Huang WJ, Niu HS, Lin MH. Antihyperglycemic effect of catalpol in streptozotocin-induced diabetic rats. *J Nat Prod* 2010, 73: 1170–1172.
15. Mao YR, Jiang L, Duan YL. Efficacy of catalpol as protectant against oxidative stress and mitochondrial dysfunction on rotenone-induced toxicity in mice brain. *Environ Toxicol Pharmacol* 2007, 23: 314–318.
16. Li X, Xu Z, Jiang Z, Sun L, Ji J, Miao J, Zhang X, *et al*. Hypoglycemic effect of catalpol on high-fat diet/streptozotocin-induced diabetic mice by increasing skeletal muscle mitochondrial biogenesis. *Acta Biochim Biophys Sin* 2014, 46: 738–748.
17. Juárez-Reyes K, Brindis F, Medina-Campos ON, Pedraza-Chaverri J, Bye R, Linares E, Mata R. Hypoglycemic, antihyperglycemic, and antioxidant effects of the edible plant *Anoda cristata*. *J Ethnopharmacol* 2015, 161: 36–45.
18. Zhou L, Yu X, Meng Q, Li H, Niu C, Jiang Y, Cai Y, *et al*. Resistin reduces mitochondria and induces hepatic steatosis in mice by the protein kinase C/protein kinase G/p65/PPAR gamma coactivator 1 alpha pathway. *Hepatology* 2013, 57: 1384–1393.
19. Putti R, Della RA. PeptideYY and insulin coexist in beta-granules in B cells of the Madagascan lizard, *Zonosaurus laticaudatus*. *Gen Comp Endocrinol* 1996, 103: 249–256.
20. Zang M, Zuccollo A, Hou X, Nagata D, Walsh K, Herscovitz H, Brecher P, *et al*. AMP-activated protein kinase is required for the lipid-lowering effect of metformin in insulin-resistant human HepG2 cells. *J Biol Chem* 2004, 279: 47898–47905.

21. Ma H, Quan F, Chen D, Zhang B, Zhang Y. Alterations in mitochondrial function and spermatozoal motility in goat spermatozoa following incubation with a human lysozyme plasmid. *Anim Reprod Sci* 2010, 121: 106–114.
22. Wang X, Jiang Z, Xing M, Fu J, Su Y, Sun L, Zhang L. Interleukin-17 mediates triptolide-induced liver injury in mice. *Food Chem Toxicol* 2014, 71: 33–41.
23. Chung MJ, Sung NJ, Park CS, Kweon DK, Mantovani A, Moon TW, Lee SJ, *et al*. Antioxidative and hypocholesterolemic activities of water-soluble puerarin glycosides in HepG2 cells and in C57BL/6J mice. *Eur J Pharmacol* 2008, 578: 159–170.
24. Bradford BL, Gerald IS. Mitochondrial dysfunction and type 2 diabetes. *Science* 2005, 307: 384–387.
25. Chen N, Leng YP, Xu WJ, Luo JD, Chen MS, Xiong Y. Contribution of endogenous inhibitor of nitric oxide synthase to hepatic mitochondrial dysfunction in streptozotocin-induced diabetic rats. *Cell Physiol Biochem* 2011, 27: 341–352.
26. Tomas J, Michael R. Mitochondrial plasticity in obesity and diabetes mellitus. *Antioxid Redox Signal* 2013, 19: 258–268.
27. Shieh JP, Cheng KC, Chung HH, Kerh YF, Yeh CH, Cheng JT. Plasma glucose lowering mechanisms of catalpol, an active principle from roots of *Rehmannia glutinosa*, in streptozotocin-induced diabetic rats. *J Agric Food Chem* 2011, 59: 3747–3753.
28. Rolo AP, Palmeira CM. Diabetes and mitochondrial function: role of hyperglycemia and oxidative stress. *Toxicol Appl Pharmacol* 2006, 212: 167–178.
29. Ferreira FM, Moreno AJ, Seiça R, Santos MS, Palmeira CM. Diabetes and mitochondrial bioenergetics: alterations with age. *J Biochem Mol Toxicol* 2003, 17: 214–222.
30. Franko A, von Kleist-Retzow JC, Böse M, Sanchez-Lasheras C, Brodesser S, Krut O, Kunz WS, *et al*. Complete failure of insulin-transmitted signaling, but not obesity-induced insulin resistance, impairs respiratory chain function in muscle. *J Mol Med (Berl)* 2012, 90: 1145–1160.
31. Franko A, von Kleist-Retzow JC, Neschen S, Wu M, Schommers P, Böse M, Kunze A, *et al*. Liver adapts mitochondrial function to insulin resistant and diabetic states in mice. *J Hepatol* 2014, 60: 816–823.
32. Sivitz WI, Yorek MA. Mitochondrial dysfunction in diabetes: from molecular mechanisms to functional significance and therapeutic opportunities. *Antioxid Redox Signal* 2010, 12: 537–577.
33. Nishikawa T, Araki E. Impact of mitochondrial ROS production in the pathogenesis of diabetes mellitus and its complications. *Antioxid Redox Signal* 2007, 9: 343–353.
34. James AM, Collins Y, Logan A, Murphy MP. Mitochondrial oxidative stress and the metabolic syndrome. *Trends Endocrinol Metab* 2012, 23: 429–434.
35. Zhang XL, Jing B, Li ZB, Hao S, An LJ. Catalpol ameliorates cognition deficits and attenuates oxidative damage in the brain of senescent mice induced by D-galactose. *Pharmacol Biochem Behav* 2007, 88: 64–72.
36. Hu L, Sun Y, Hu J. Catalpol inhibits apoptosis in hydrogen peroxide-induced endothelium by activating the PI3 K/Akt signaling pathway and modulating expression of Bcl-2 and Bax. *Eur J Pharmacol* 2010, 628: 155–163.
37. Bi J, Jing B, Liu JH, Lei C, Zhang XL, An LJ. Protective effects of catalpol against H_2O_2-induced oxidative stress in astrocytes primary cultures. *Neurosci Lett* 2008, 442: 224–227.
38. Fischer F, Hamann A, Osiewacz HD. Mitochondrial quality control: an integrated network of pathways. *Trends Biochem Sci* 2012, 37: 284–292.
39. Jang YY, Song JH, Shin YK, Han ES, Lee CS. Protective effect of boldine on oxidative mitochondrial damage in streptozotocin-induced diabetic rats. *Pharmacol Res* 2000, 42: 361–371.
40. Tao R, Coleman MC, Pennington JD, Ozden O, Park SH, Jiang H, Kim HS, *et al*. Sirt3-mediated deacetylation of evolutionarily conserved lysine 122 regulates MnSOD activity in response to stress. *Mol Cell* 2010, 40: 893–904.
41. Ricquier D, Bouillaud F. The uncoupling protein homologues: UCP1, UCP2, UCP3, StUCP and AtUCP. *Biochem J* 2000, 345: 161–179.
42. Krauss S, Zhang CY, Lowell BB. The mitochondrial uncoupling-protein homologues. *Nat Rev Mol Cell Biol* 2005, 6: 248–261.
43. Lee SC, Robson-Doucette CA, Wheeler MB. Uncoupling protein 2 regulates reactive oxygen species formation in islets and influences susceptibility to diabetogenic action of streptozotocin. *J Endocrinol* 2009, 203: 33–43.
44. Scheibye-Knudsen M, Fang EF, Croteau DL, Wilson DM, Bohr VA. Protecting the mitochondrial powerhouse. *Trends Cell Biol* 2015, 25: 158–170.
45. Bach D, Pich S, Soriano FX, Vega N, Baumgartner B, Oriola J, Daugaard JR, *et al*. Mitofusin-2 determines mitochondrial network architecture and mitochondrial metabolism. *J Biol Chem* 2003, 278: 17190–17197.
46. Ansgar S, Stephan F, Brigitte G, Michael H. Mitofusin-1 protein is a generally expressed mediator of mitochondrial fusion in mammalian cells. *J Cell Sci* 2003, 116: 2763–2774.
47. Yu T, Robotham JL, Yisang Y. Increased production of reactive oxygen species in hyperglycemic conditions requires dynamic change of mitochondrial morphology. *Proc Natl Acad Sci USA* 2006, 103: 2653–2658.
48. Mahendra PB, Lim YC, Kim YM, Ha KS. C-Peptide activates AMPKα and prevents ROS-mediated mitochondrial fission and endothelial apoptosis in diabetes. *Diabetes* 2013, 62: 3851–3562.